Structural cast glass components manufactured from waste glass
Diverting everyday discarded glass from the landfill to the building industry

Bristogianni, Telesilla; Oikonomopoulou, Faidra; Justino de Lima, Clarissa; Veer, Fred; Nijsse, Rob

Publication date
2018

Document Version
Final published version

Published in
Heron

Citation (APA)
Bristogianni, T., Oikonomopoulou, F., Justino de Lima, C., Veer, F., & Nijsse, R. (2018). Structural cast glass components manufactured from waste glass: Diverting everyday discarded glass from the landfill to the building industry. *Heron*, *63*(1/2), 57-102. Article 4.

Structural cast glass components manufactured from waste glass: Diverting everyday discarded glass from the landfill to the building industry

Telesilla Bristogianni [a], Faidra Oikonomopoulou [b], Clarissa Justino de Lima [a], Fred A. Veer [b], Rob Nijsse [a,b]

[a] TU Delft, Faculty of Civil Engineering and Geosciences, the Netherlands, t.bristogianni@tudelft.nl

[b] TU Delft, Faculty of Architecture and the Built Environment, the Netherlands

Although in theory glass can be endlessly re-melted without loss in quality, in practice only a small percentage gets recycled, mainly by the packaging industry. Most of the discarded glass fails to pass the high quality standards of the prevailing glass industry – due to coatings, adhesives, other contaminants or incompatibility of the recipe – and ends up in landfill. However, using discarded glass in cast components for building applications can be a good way to reintroduce this waste to the supply chain. Such components can tolerate a higher percentage of inclusions, without necessarily compromising their mechanical or aesthetical properties. This paper explores the potential but also the limitations of recycling glass in order to obtain load-bearing components. First, an overview is provided regarding which types of glass reach the recycling plants and which not, arguing on the reasons behind this selection. Afterwards, a series of experiments is presented, exploring the possibilities of recycling everyday glass waste, from beer bottles and Pyrex trays to mobile phone screens. Each type of glass waste is cast at different temperatures and firing/cooling rates to define its flow capability and risk of crystallization. The above information is linked to the X-ray fluorescence (XRF) analyses of the samples prior to recycling. The results point out the types of glass with potential in structural applications, and the overall feasibility of the concept. This paper is an extension of previously reported work by Bristogianni et al. 2018.

Keywords: Glass waste, glass recycling, cast glass components, kiln-casting, crystallization

1 Introduction

The term glass recycling is almost a synonym to the sole recycling of glass bottles and containers for the purposes of the food packaging industry. The glass packaging industry has significantly invested in the infrastructure for the collection, sorting and processing of glass bottle and container waste, and this has resulted in high percentages of waste recovery and recycling, such as a mean of 73.2% in 2015 in the European Union (Eurostat 2016). Glass waste is however a broader term including overall everyday household waste (ex. tableware, ovenware, lighting), building waste (ex. windows, glass tiles), electronic waste (ex. Liquid Crystal Displays and Cathode Ray Tubes), automotive industry waste (ex. laminated windshields) and industrial/laboratory waste to name a few. The percentages of recovery and recycling of non-packaging glass waste are rather low, effectively zero (ELVIROS 2004). Such glass objects are considered non-recyclable either due to contamination from coatings, adhesives, laminates or even hazardous substances, or due to the labour intensive demounting process required (ex. window panes, computer screens) (Dyer 2014). The food packaging industry does not accept contaminated glass cullet that will affect the taste of the products, same as the float industry rejects such glass, as it is responsible for the creation of stones and other flaws and reduces the transparency of their glass panes while also increasing the risk of failure due to inclusions such as Nickel Sulfide (NiS). Since this glass cannot meet the strict criteria to be reused for the same purpose (close-loop recycling), it either ends up in landfills or gets down-cycled (open-loop recycling) into aggregate in concrete, ceramic or pavement products, into abrasive or into foam insulation (Silva et al. 2017; Dyer 2014). What is more, tons of non-contaminated glass waste are simply discarded or down-cycled due to the mismatch in their recipe with that of glass packaging. In other words, the lack of facilities and automated processes for separation and handling of different types of glass is- at a great extend- responsible for the rejection of this waste from the close-loop recycling.

Cast glass technology for structural applications can be a strategy for tackling the problem of glass waste rejection due to contamination or glass composition. Cast glass has already been applied in load-bearing applications, such as the self-supporting glass façade of the Crystal Houses in Amsterdam (Oikonomopoulou et al. 2017). On the one hand, building

components out of cast glass can tolerate more flaws[1] than a piece of float glass or a drinking bottle, without compromising the strength or aesthetic quality. On the other hand, the relatively smaller scale of the cast glass factories and often lack of automation leave more room for experimentation. In contrast to the giants of glass processing and their strict specifications, cast glass producers have more freedom in altering the firing schedules and the glass recipes.

Scope of this paper, is the categorization of prevailing types of glass waste and the understanding of their value as a raw source for the casting of glass building components. Not only the mechanical properties of the final product are important, but also the suitability and easiness of a waste glass type to be cast in the first place. To elaborate on the aforementioned suitability, it should be noted that for each composition, a different liquidus temperature region and minimum cooling rate apply. These parameters need to be taken into account during casting in order to obtain glass, or in other words, to freeze the amorphous structure of the liquid melt into the solid component. A glass formed at temperatures just below this region and cooled down at slower rates, bares the risk of crystallization (Pye 2005). As a consequence, according to the heating and cooling conditions, a portion or all the material will be structured in crystals, and the end product will have altered properties. Such crystallized materials, for example, lose the property of transparency and become more impact resistant than their amorphous alternative (Cormier 2017). Therefore, the parameters defining each type of glass waste should facilitate the casting process, implying that high liquidus temperatures or extremely fast cooling rates are not realistic for the mass production of building components of a competitive price.

[1] Experimental testing on cast glass components at the TU Delft Glass & Transparency Lab indicate that a few air bubbles or inclusions (ex. ceramic stones) within the bulk of the components- that do not exceed a diameter of a millimeter- are not critical for the structural performance Similar bubbles or stones in a glass pane of 6/8 mm thickness would significantly reduce the strength of the product, but also its aesthetic quality (a perfectly clear transparent pane is expected). For similar aesthetic reasons, colour shifts are rejected from the industry and consumers, but can be of aesthetic value in cast glass elements.

2 Categorization of everyday glass waste

2.1 Prevailing glass families

By clustering the commercial glass waste into families of similar chemical composition, we can set guidelines on how to handle each piece of glass waste and what to expect from the resulting product. In specific, we can define the working and annealing temperature range, the easiness of crystallization, the coefficient of thermal expansion and the possibility of combination with similar glass waste sources. We can also predict the characteristics of the finished products in terms of mechanical, optical and thermal properties.

Everyday glass waste was therefore categorized in the following six families: soda-lime, soda-potash-lime, lead crystal, lead-free crystal, borosilicate and alkali-aluminosilicate glass. Within the soda-lime category- which is also the most prevailing one- three subcategories were set in relation to the manufacturing process of the glass objects, since the production method fine tunes the basic soda-lime recipe. These subcategories are: automated blown, mouth-blown and float glass. Other types of specialty glasses are not included in this research as their contribution to the problem of glass waste is negligible.

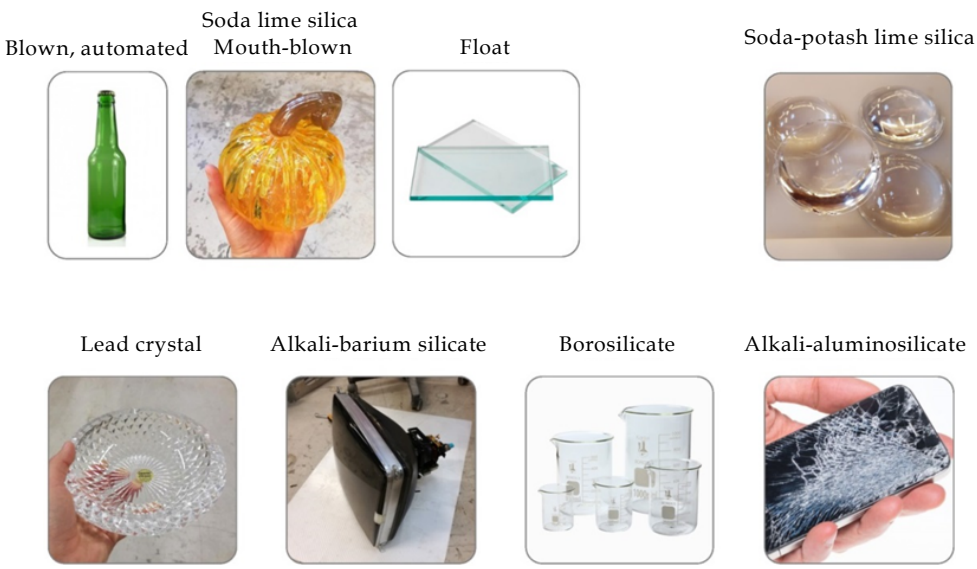

Figure 1: Main families of commercial glasses

Appendix 1 provides a list of properties for each family of commercial glass. This list has been used in this research as a guideline for determining the handling temperatures during the casting of the different glass waste.

2.2 Selection of glass waste samples

According to the above categorization, characteristic samples from each type of glass family were collected and analyzed with a Panalytical Axios Max WD-XRF spectrometer in order to define their glass composition. The Panalytical set of Omnian standards were used for calibration, as well as several NIST SRM standards and pure (p.a.) compounds. The results can be seen in Appendix 2. In short, the following samples were analyzed per category:

- Soda lime/ blown, automated: Beer/wine/soda bottles, drinking glasses
  - Soda lime/ mouth-blown: artefacts from the glass blowing studio at Southern Illinois University
  - Soda lime/ float: window glass, waste glass from furnace clean-up
- Soda-potash lime: optical lenses, tableware
- Lead crystal: tableware
- Lead-free crystal: CRT screen (panel)
- Borosilicate: laboratory tubes
- Alkali-aluminosilicate: mobile phone screen

3 Recycling experiments and interpretation of the results

3.1 Experimental set-up

In this section, an explanation of the set-up parameters is provided. Regarding the casting method for the sample production, the two techniques listed below were followed, according to the maximum operating temperature needed:

a) Kiln-casting employing investment silica-plaster moulds. For this method, one kiln is used for the melting and annealing of the glass and therefore, the feeding of the moulds with glass takes place inside the kiln. Three different types of moulds were produced:

- Crystalcast M248, powder to water volume ratio 2.75 : 1. The product consists of cristobalite, quartz and gypsum (Gold Star). For firings above 1000°C, the crystalcast moulds are reinforced by an exterior layer of heat-resistant concrete.

- Ransom & Randolph (R&R) Glass Cast 910, powder to water mass ratio 10 : 2.8. The product consists of cristobalite, quartz, mullite, calcium sulfate and fibrous glass (Ransom & Randolph).
- Heat-resistant concrete coated with a 1mm thick layer of Mold Mix 6 by Zincar, which is a high alumina putty coating with glass reinforcement fibers (ZRCI 2017). Two layers of EKamold® spray are applied as top coating. This product is an ethanolic coating based on hexagonal boron nitride (ESK 2013). This mould was used for a firing at 1250°C.

The glass was introduced in the moulds either directly ("free-set") or indirectly by being placed in terracotta flowerpots that were positioned above the moulds. The heating ramp was set at 50°C/h. Regarding the quenching applied to prevent the crystallization of the components, the samples are either manually quenched below their softening point, by opening and closing the kiln door in repetition or mechanically by setting the kiln controller at the "As Fast As Possible" (AFAP) function. The later cooling process requires more time versus the manual, abrupt quenching.

a) *b)* *c)*

Figure 4: a) Kiln-casting in Crystalcast moulds with glass directly placed in the moulds (free-set), b) Kiln-casting in Crystalcast moulds employing the flowerpot technique, and c) Hot pouring in steel mould.

b) Melt-quenching technique employing high-alumina crucibles and steel moulds. This method is preferred in this research for castings above 1250°C, due to the high thermal and chemical resistance of the alumina crucibles. For this method, two kilns are needed for the

melting and annealing of the glass respectively. The glass is molten in Coors™ high-alumina crucibles and poured at atmospheric conditions in steel moulds that are preheated at 500°C. Upon quenching, the samples are placed in the annealing oven together with the steel mould. The heating rate used was 17.5°C/min.

*3.2 **Casting experiment of the selected glass waste families***

Samples were cast from six selected glass families at different temperatures. The samples are initially evaluated on their workability. As the collection of samples includes glasses that have been developed for other production techniques (automated-blowing, float line, automated draw etc.), implications are expected when attempting to cast them, especially with the- slower- method of kiln-casting. Ideally, the glass samples should be able to flow and homogenize at temperatures below 1000°C, both to increase the energy savings but also to simplify the prerequisites of their mould. Aim of the research is thus to identify the glasses that have both lower working temperatures and a resistance to crystallization from the glasses that are difficult to cast and which will need extra attention. For this identification step, each glass is cast individually. The following observations and conclusions can be gathered for each glass family:

• *Soda lime/blown, automated (Container glass such as beer/wine/soda bottles, drinking glasses)*

These glasses are developed for the automated blowing process, therefore they need to be stiff enough to keep their shape once blown in a mould. Although this prerequisite decreases the workability of the glass, this fact is counteracted by the mechanically applied air pressure for the moulding. This attribute was prevailing during the casting of these glasses, since the samples needed temperatures higher than 1000°C in order to flow and homogenize. Moreover, all samples were very susceptible to crystallization below the liquidus temperature. Abrupt quenching was necessary to avoid full crystallization and to confine the problem only to the top surface. More specifically, samples cast at 860°C would not flow but only partially fuse, and would appear fully crystallized with mechanical quenching. At 950°C the drinking glass sample failed to homogenize and crystallized despite its fast cooling. Likewise, the samples cast at 970°C and mechanically quenched were crystallized and incomplete, as the glass could not easily flow from the flowerpot down to the mould. It should be noted, however, that samples appearing to be fully crystallized, proved to contain glassy zones within their body, when sliced in two and observed along their cross section. Only when cast at 1120/1200°C and abruptly cooled down to 600°C were the resulting samples transparent. This transparency was evident after

a) *b)* *c)*

d) *e)* *f)*

Figure 6: a), b) Beer bottle starting to fuse inside the flowerpot, at 860°C, c) drinking glass, crystallized at 950°C, d) beer bottle fused inside the flowerpot and partially crystallized, e) clear bottle cast at 1200°C with top surface crystallization linked to the contact of the glass to the mould, f) beer bottle cast at 1200°C.

the top crystallized surface[2] and the bottom surface in contact with the investment mould were polished.

From the XRF data obtained, we can observe that all above tested glasses have a similar composition. Mainly we see a range of 71.12 – 73.99 per weight percentage (wt%) of SiO_2, 10.95 – 12.90 wt% Na_2O, and 9.74 – 11.88 wt% CaO. Calcium oxide (CaO, lime) is increasing the softening point and the sagging temperature, thus the observed high viscosity of the samples (Zschimmer 2013). Although this is required for the automated

[2] Unless a nucleating agent is added in the glass melt to promote bulk crystallization, usually crystallization starts from the glass surface. Airborne dust is often the main trigger. In addition, volatilization of various components from the glass melt alters the composition at the outer layer. Particles from the mould found on that altered surface could also act as nucleating sites (Müller 2000).

blowing process, the increased softening point impediments the casting. The high percentage of lime is also responsible for the susceptibility to crystallization. According to Zschimmer, lime percentages above 10% promote devitrification. This is to be taken into account when working with this glass sub-family.

It should be also mentioned that although the tested glasses have almost the same composition and viscosity, their colour is affecting their setting time. Kitaĭgorodskiĭ et al. (1934) and Burch et al. (1938) proved that glasses with identical basic composition and viscosity characteristics, differ regarding their working range. In specific, dark coloured glasses, due to their greater heat loss by radiation rate, tend to set much faster than the equivalent transparent or light coloured samples. Holscher et al. (1943) suggest chromium emerald green glasses of basic composition SiO_2 74.0 wt%, Na_2O 16.0 wt%, CaO 10.0 wt%, Fe_2O_3 0.035 wt% and Cr_2O 0.25 wt% to be one of the most rapid cooling systems after dark green Fe-Mn systems. In our tested samples that could be easily verified by the intense luminosity of these samples at 1200°C in comparison to the transparent ones. The fast setting of darker colours should be considered when the hot-pouring method is employed.

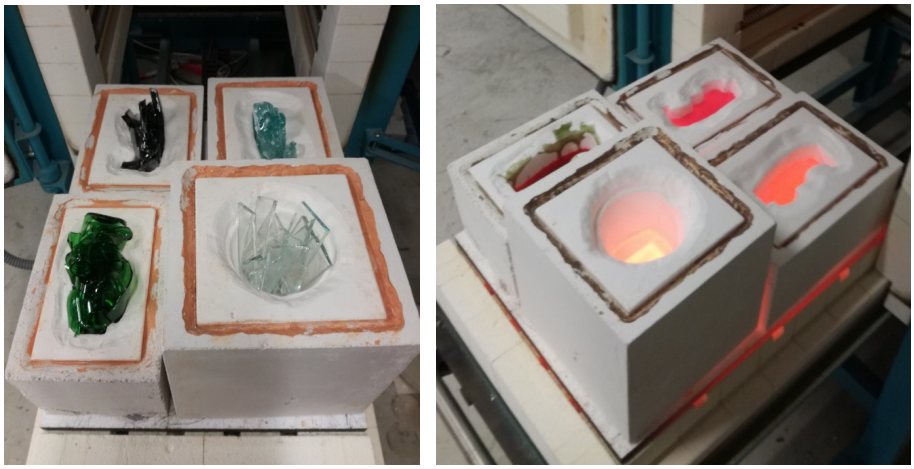

Figure 7: Kiln-casting experiment at 1120°C, portraying the differences in luminosity among the various coloured samples

Experiments with mixing different container samples together were also conducted in order to define their compatibility. The glass recycling industry separates soda-lime containers from numerous different producers into similar colours. The segregated cullet is then successfully recycled together with new raw material. In that sense, casting two

different clear bottles together was expected to work well at temperatures corresponding to viscosities of $10^{1.5\text{-}2.5}$ poise, which are achieved in the melting tanks. For typical soda-lime silica glasses (Kimble R-6 used as reference), a $10^{2.5}$ viscosity would correspond to 1254°C (Martlew 2005). Therefore it was opted to test the combination at a lower temperature, namely 970°C. The sample, placed in a flowerpot, was kept at top temperature for 2 hours and then mechanically quenched. A small part of the glass mixture flew down the mould and despite the fact that the glass was fully crystallized, it was homogenized and did not crack during annealing. Regarding the glass mass that remained in the flowerpot, this could be observed by cutting the pot in half. There, zones of crystallized glass of almost same thickness (similar to the thickness of the bottles) are fused

a) Droplets that flowed from the flowerpot down to the mould

b) Glass part that fused inside the flowerpot. In this picture, the surface in contact with the flowerpot is seen

c) Flowerpot cut in half, showing the layering of the fused glass and the glassy areas within the crystallized mass.

Figure 8: Results of the kiln-casting of two different types of clear bottles at 970°C

together. A few glassy regions are also observed. It is interesting to see that the zone of glass in contact with the flowerpot – which heats up and cools down faster – is more homogeneous and has a different micro-pattern of crystallization.[3] Regardless of the

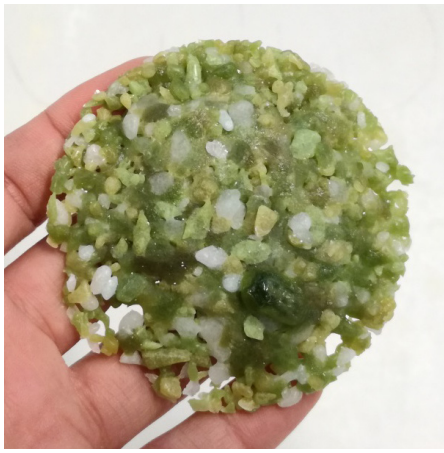

a) 970°C (small shards)

b) 970°C (powder)

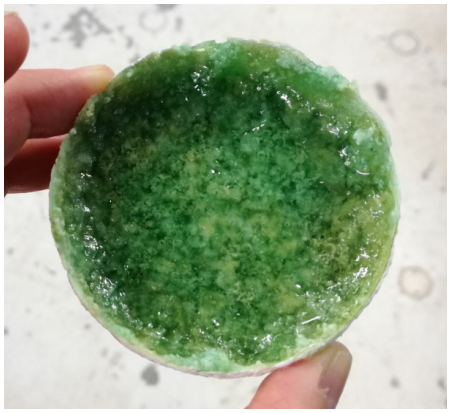

c) 940°C (powder + flux)

d) 1250°C (powder)

Figure 9: Samples of different coloured glass bottles kiln-cast

[3] In comparison to the previously described high temperature tests at 1200-1250°C, in this case the glass shards reach a state just above the softening point that allows them to compact within the flowerpot. Moreover, there is a difference observed within the bulk of each individual shard and its exterior surface. The bulk is overall cooler than the exterior surface and has a high viscosity that acts as a kinetic barrier for the formation of crystals. The exterior, however, heats up first and has a reduced viscosity that allows the fusion with the adjacent shards. This viscosity simultaneously allows the formation of crystals, thus the crystallization observed in these areas.

above, none of the glass masses cracked, proving that this combination is also feasible at temperatures below 1250°C.

The mixing of different colours of container glass (wine bottles) was also tested, in various sizes from powder to small and medium sized shards. The XRF analysis of 4 different samples showed strong compositional similarity despite the colour shifts. The mix of wine bottles was fired at various temperatures between 940°C – 1450°C. At 970°C the sample would partially fuse and still keep the integrity and colours of the individual pieces. This comes in antithesis with the above mixture of clear bottles (similar recipes to the wine bottles) that homogenized at the same temperature. In this case, the differences in colour/exact recipe, seem to require higher temperatures. Nonetheless, the sample did not crack upon annealing. Adding 10% of fluxing agent (in this case CNa_2O_3) in the powdered mix and firing it at 940°C helped the melting of the top surface but did not result in a homogenized sample. The sample was homogenized at the tests conducted from 1200°C and above. Higher temperatures are required for the homogenization of this combination.

In general, despite the challenges to cast this sub-family described in this chapter, glass container waste is still the most prevailing one. In that sense, it is worth exploring the derailing of sorted – yet discarded by the packaging industry – glass waste, from the landfill to the building sector. As an advantage, the iron in the green and amber (combined with Sulfur) glasses can provide excellent UV-radiation protection (Shelby 2005) and should thus be considered for use in facades.

• *Soda lime/ mouth-blown (artefacts from the glass blowing studio at Southern Illinois University)*
Glass studios, either commercial or academic, produce quite some glass waste during their trial and error explorations. Especially the discarded pieces by the glassblowing hotshop containing colour are not reused for blown objects, as this would imply the contamination of the clear transparent batch in the furnace.

In contrast to the above glass category, these glasses are meant to be processed according to the power of the human lung, therefore they cannot be as stiff. Also, the artists require a prolonged working time to process their piece, thus a glass that will not set as fast as the container glass. Correspondingly, the content of lime (CaO) in this composition is found around 6.8-7.1 wt% and of sodium oxide (Na_2O) at 14.3-15.4 wt%. The glass samples thus could slowly flow down from the flowerpots to the moulds at 860°C, a temperature

considerably lower than the one necessary for the machine-blown glass objects of the same glass family. However, the lack of abrupt quenching can still induce extended crystallization in the samples. The differences in the working range between the various colour variations are valid also here. Overall though, these coloured glasses are usually engineered to be compatible and as a result beautiful colour patterns can emerge from their combination. Crystallized samples can lead as well to interesting marble-like smooth components. Since the mechanical properties of these objects are expected to be improved during the devitrification, experimental testing of their strength is required in follow-on research, in order to explore their potential value as building components.

Figure 10: Set-up of the kiln and glass ceramic samples resulting from the mouth-blown glass waste

Figure 11: Glass samples cast employing Sprucepine clear and blue glass waste (top and bottom) and lead crystal (middle element). The figure shows the effect of casting temperature to the structure of the glass component. Although the top and bottom sample are cast using the same glass, the one below, cast at 860°C crystallized, in comparison to the clear blue component on top, cast at 950°C.

Further investigation on the crystallization issue of these samples showed that a relatively slow cooling rate is not as decisive as the choice of top temperature for kiln-casting. Using transparent clear and blue Sprucepine shards, two elements were cast, one at 860°C and one at 950°C, kept at top temperature for 10 hours and then cooled down to annealing point with a rate of 120°C/h. The sample cast at a lower temperature appeared fully crystallized in comparison to the one cast at a higher temperature, which resulted in a transparent blue glass.

In order to explain this observation and define the dangerous crystallization zone of this glass, a comprehensive glass thermal analysis (Differential Scanning Calorimetry DSC) was performed to a sample of transparent clear Sprucepine glass, employing a STA 449 F3 Jupiter® apparatus.

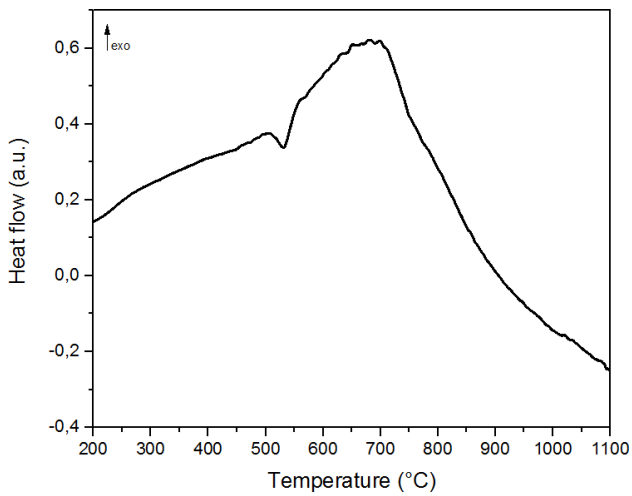

Figure 12: DSC analysis pointing out the glass transition temperature and crystallization peak temperature of Spruce Pine transparent clear glass

The DSC analysis defines the crystallization peak at around 700°C. Observing the endothermic process after this point, we can notice the drastically fall of the DSC curve. This proves that there is a significant difference between casting this glass at 860°C and 950°C.

Regarding the crystallized sample cast at 860°C, the extent of crystallization was also questioned, especially after observing the remaining glass mass in the flowerpot used for

its casting. There, the existence of both crystalline and glassy phases is evident. Therefore, an X-ray diffraction (XRD) test was conducted, employing a Bruker D8 Advance diffractometer Bragg-Brentano geometry and a Lynxeye position sensitive detector.

Figure 13: Glass sample from the flowerpot used during the 860°C casting experiment, showing the formation of crystals

Table 1: Results of the XRD analyses for samples cast at 950 and 860°C. The samples are taken from the top surface of the components and not from the remaining glass in the flower pots.

Sample		Top temp. *)	Transparency	Crystalline phases	Compound	%
1		A 950°C	Transparent	No	-	0
2a		B 860°C	Transparent with opaque zones	Sodium Calcium Silicate	$Na_2Ca_3Si_6O_{16}$	≈ 3
2b		B 860°C	Opaque	Sodium Calcium Silicate	$Na_2Ca_3Si_6O_{16}$	≈ 10

*) The firing quench ramp was 120°C/h

The XRD analyses identified the presence of crystalline phases in the sample cast at 860°C. In specific, the sodium calcium silicate component $Na_2O.3CaO.6Si0_2$ was found, also known as devitrite. Devitrite is a common crystallization product of soda-lime-silica glasses (Clark-Monks et al., 1980). Interestingly enough, although the sample appeared as

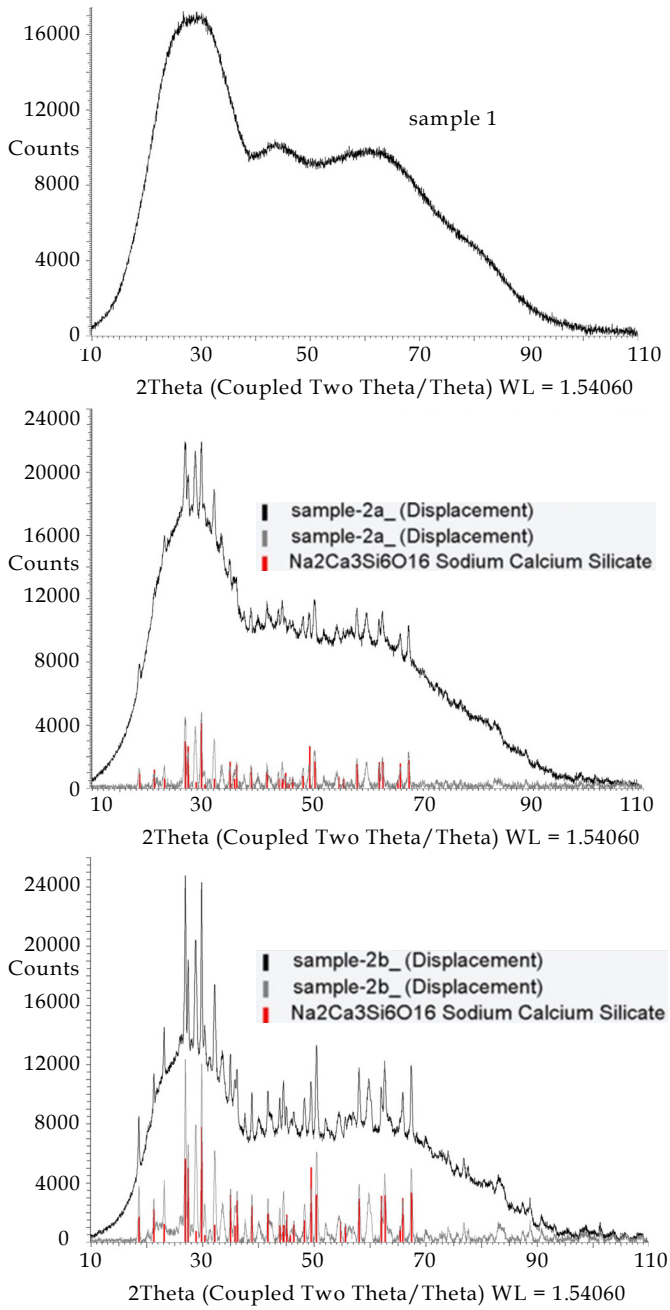

Figure 15: The XRD graph shows the measured patterns in black, after background subtraction. The coloured bars give the peak positions and intensities of the possibly present identified phases, using the ICDD pdf4 database. All samples are amorphous but some have a small fraction of crystalline phases.

fully crystallized (the exterior surface is completely opaque and clusters of crystal patterns are visible), not more than 10% of its structure was crystalline. The sample taken from the 950°C specimen, was entirely amorphous. Further experiments need to be conducted to determine how the crystalline percentage can be controlled and what the effects are of these percentages on the structural strength of the components.

• *Soda lime/ float (window glass, waste glass from furnace clean-up)*

The float glass samples present a bit higher weight percentages of SiO_2 74, 21-74, 56 and Na_2O 12, 44-13, 32 and lower CaO percentage of 8.91-10.03 in comparison to the automated-blown glass. Magnesium Oxide (MgO) levels are also higher by 1-1.5 wt%. The XRF analysis was conducted at only one surface of the samples which is assumed to be the top surface since no contamination by the tin bed is observed. The glass would be very viscous at 860°C, flowing very slowly. Full crystallization occurred by mechanical quenching at the extra clear sample (PPG Starphire). These glasses could be cast homogeneously at 1200°C and presented only surface crystallization with abrupt cooling.

Here the difference in the crystallization pattern between the clear and the extra clear float samples should be mentioned. The clear sample presented a subtle translucent finishing at the top surface and a couple of local areas of mild crystal formations. The extra clear (PPG Starphire) glass however, showed a more intense crystallization pattern at the top surface, with visible crystal clusters.

It is not clear – when comparing the two glass compositions – why the extra clear sample is more prone to crystallization, but this could also be related to a possible contamination of the top surface from the tin bath. An XRF analysis of the cast sample should be conducted to further investigate this. To better define the extra clear glass, a comprehensive glass thermal analysis (DSC) was performed. The test showed a stable glass, but with a crystallization peak at around 740°C. The glass transition temperature was found at the region of 570°C. With proper cooling- fast enough to avoid the crystallization at the above mentioned peak- this glass can result into very clear and transparent castings.

Regarding the waste from the float production furnace clean-up, this refers to glass that may be located at the bottom of the furnace for years. The glass slowly decays the refractory materials at the base and absorbs part of their elements in its composition. The resulting glass- although in rough lines similar in composition to the original soda-lime

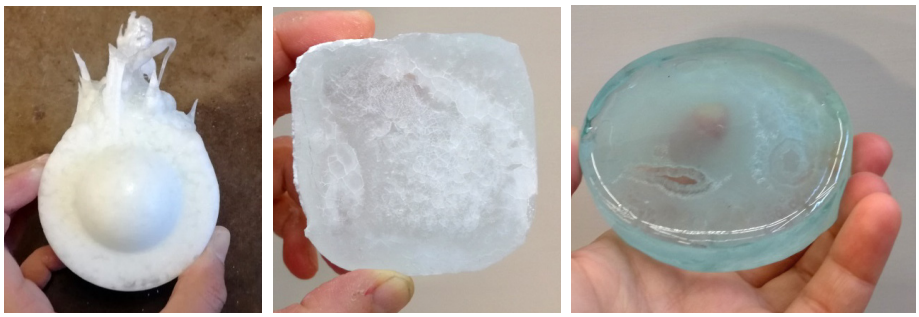

Figure 16: PPG Starphire kiln-cast at 860°C and mechanically quenched (left), PPG Starphire sample kiln-cast at 1200°C with top surface crystallization (middle), PPG clear float sample kiln-cast at 1200°C (right)

Figure 17: PPG furnace waste aquamarine cast at 1120°C (left) and at 860°C (middle). PPG Starphire cast at 1120°C (right)

one, can be quite unpredictable in its exact composition and therefore in its casting behavior. For example, the "PPG light green waste glass" was a very viscous glass (could not flow at 860°C) but also extremely resistant to crystallization. The increased viscosity can be explained by the high content of alumina (8.8 wt%). According to Zschimmer (2013), although alumina reduces the melting point of soda-lime-silica glasses when introduced in small amounts, in weight percentages of more than 7% it has the opposite effect. The increased alumina content in combination with the relatively low percentage of lime (5.94 wt%) is what makes this glass so resistant to crystallization. It is also interesting to point out the content of 2.98 wt% of zirconia (ZrO_2) in combination with traces of hafnia (HfO_2). Zirconia is a refractory material found as paving on the furnace bottom (Clark-

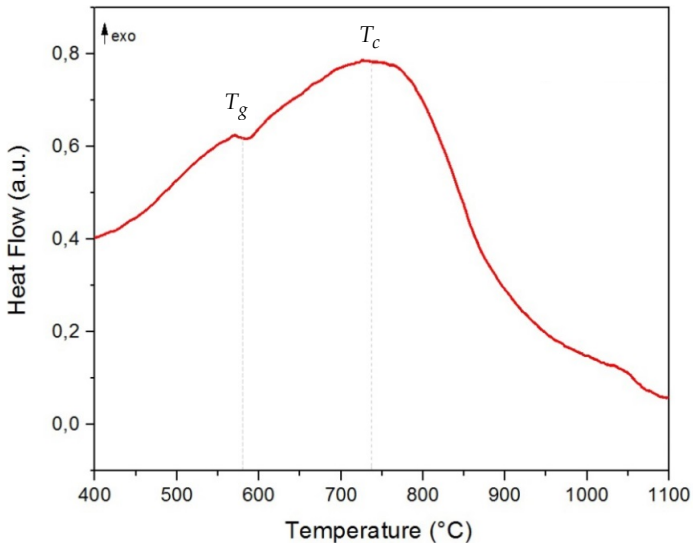

Figure 18: DSC analysis pointing out the glass transition temperature and crystallization peak temperature of PPG Starphire

Monks et al. 1980), especially in cases where very corrosive glasses are melted (Bray et al. 2001). Moreover, Alumina-Zirconia-Silica (AZS) refractories are often used by the glass industry in favour of high-alumina refractories, which tend to more easily corrode and release alumina in the molten glass (Bray et al. 2001). The usage of such refractory products can explain the high content of this glass in alumina and zirconia. Zirconium minerals contain hafnium, in a range of 1.5 - 2.5%Hf/Zr+Hf or more (Nielsen 2000), justifying the traces of hafnia in this glass. Karell et al. (2007) mention that zirconia increases the viscosity of the melt- as observed- but is also used as a substitute to PbO in lead-free crystal glasses, as it increases the refractive index of the glass and thus the light dispersion. The later information can be linked with the high optical quality of the cast sample.

The "PPG furnace waste aquamarine" sample did not exhibit serious contamination from the refractory materials and had a composition very close to that of standard float glass. At 860°C the sample was viscous but could only flow slowly. By inducing mechanical cooling, partial crystallization occurred, with some glassy amorphous regions still preserved within its mass. The same glass could be cast homogeneously at 1120 and 1200°C and presented minor surface crystallization as did sample "PPG clear".

Green glass before and after casting at 860°C

Aquamarine glass cast at 860°C and 1200°C respectively

Figure 19: PPG furnace waste glass

Despite the unpredictable character of this type of glass waste, interesting colours and patterns can emerge from the casting of these – enriched through their prolonged contact with the furnace – glasses.

• *Soda-potash lime (optical lenses, tableware)*

Potassium oxide (K_2O) is often added in soda-lime-silica systems to achieve extra white clear glass (Zschimmer 2013). K_2O lowers the melting point of the glass yet increases the thermal expansion coefficient. Such alkali-lime silica systems containing considerable amounts of soda and potash and reduced amounts of lime are preferred for hand-pressing, since these glasses are soft and easy to adapt to the shape of the steel mould while still viscous (Rosenhain 1908). In this category, the optical glass B270 by Schott is used as a reference, since the authors have continuously experimented with this glass due

to its good optical qualities and workability at 950°C (Bristogianni et al. 2017). A complete replacement of soda by potassium oxide is found in the pressed historical Bohemian crystal artefacts (Rosenhain 1908). Contemporary Czech (or formerly Czechoslovakian) glass pressed objects however- like the one tested in the scope of this research, may contain considerably less percentages of K_2O, and more soda and silica. The glass obtained after firing at 950°C was transparent and extra clear, yet presented intense creasing at the top surface. Possibly, a small increase in temperature would result in a better quality casting.

Figure 20: Czech glass cast at 950°C. Post-processing is required to remove the shrinkage of the top surface and reveal the actual transparent glass.

• *Lead crystal (tableware)*

Lead silica glass was a glass type commonly used for high quality table and ornamental ware before the use of lead (II) oxide (PbO) was restricted due to its toxicity. This composition was preferred by the manufacturers because of the high refractiveness that the PbO would attribute to the glass, adding brilliancy to the glass artefacts (Rosenhain 1908). Shelby (2005) explains that due to the relatively weakness of the Pb-O bonds caused by the low field strength of the large Pb^{2+} ions, the lead-silicate network can be easily disrupted. This justifies the low glass transformation temperature of this glasses. As these glasses are relatively soft, they are selected by manufacturers, when complicated manipulations during production are required (Rosenhain 1908). Lead glasses also have X-ray protective properties, which increase with the increase of lead content, and are independent from the radiation quality (Singer 1936). Yet, PbO lowers the Young modulus and the hardness of the glass and significantly increases the density (Zschimmer 2013),

factors that should be seriously considered when evaluating the use of such glasses for structural applications.

In this category, Schott LF5 (≈ 36 wt% PbO) and Gaffer G210 (≈ 44 wt% PbO) lead crystal are used as a reference in the XRF analyses, as the authors have previously conducted successful castings at 860°C, achieving extra clear glass without crystallization upon mechanical cooling. The tested sample was a pressed crystal bowl of lower lead content (≈ 24 wt%), which is a typical percentage for such tableware. The glass was successfully cast at 950°C to a clear glass without crystallization (upon abrupt quenching). At this temperature, the sample is expected to have a much lower viscosity in comparison to soda-lime glass. Yet it is interesting to mention that patterns from the initial design of the bowl were preserved at the bottom of the sample in combination with creasing at the top surface. More experiments are required to determine the flowability of this glass at this temperature, but nonetheless this glass can result to very transparent castings.

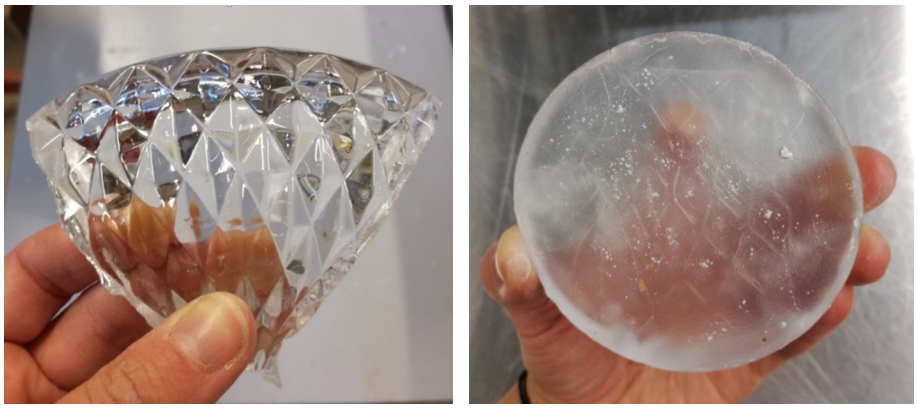

a) *Before casting* b) *After casting*

Figure 21: Pressed crystal glass cast at 950°C. The pattern of the glass remained as a trace at the bottom surface of the sample. Upon post-processing, the glass will be transparent.

• *Lead-free crystal (CRT screen/panel)*

Due to the health and environmental concerns linked with the toxicity of lead and other heavy metals, various protocols have been issued around the world with the aim to reduce its use. Regarding glass manufacturers, they would chose PbO either to increase the refractive index adding brilliance to the glass, or to provide radiation protection in nuclear plants, hospitals, TV-tubes etc. Currently, lead is replaced with barium, strontium and

zirconium, although some of the alternative elements (barium in particular) can be quite toxic themselves, only less than lead (Scoullos et al. 2001). The resulting glasses present good optical quality, lower density than lead crystal, and x-ray shielding capacity which is however reduced and dependent on the X-ray quality (Singer 1936).

In this section, the casting of the panel of a colour display Cathode Ray Tube (CRT) is attempted. CRT tubes have been used in TV and computer screens before the emergence and dominance of Liquid-Crystal Display (LCD) technology. Although currently scarcely in use, CRT glass waste constitutes an accountable percentage of the municipal waste in the European Union (Hreglich et al. 2001; Bernando et al. 2005). Since CRTs are not in production anymore, the route of their recycling into the same product is closed, leaving a question mark on how and where this glass can be used (Edgar et al. 2008). Nonetheless,

a) Screen shard *b) Top surface crystallization of the sample cast at 950°C* *c) Transparent grey glass after being post-processed*

Figure 22: CRT panel as retrieved from a computer screen

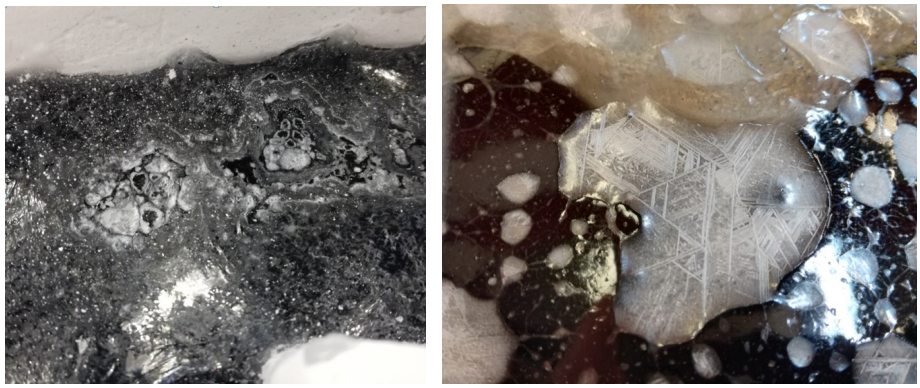

a) Kiln-cast at 1120°C *b) Kiln-cast at 970°C*

Figure 23: Surface crystallization of CRT panel glass

the glass formulation for the CRTs is of fine quality, employing – among others – expensive barium (Ba) and strontium (Sr) oxides (Compton 2003; Bernando et al. 2005). More specifically, a typical CRT tube consists of three parts: the faceplate (panel), funnel, and neck tubing. The panel, in specific, is a lead-free barium–strontium glass that protects the viewers from the harmful X-rays (Compton 2003).

A sample of a CRT panel was successfully cast at 950°C, resulting in a clear, homogeneous glass of grey hue that did not crystallize upon abrupt quenching. Indeed, this glass composition, rich in Ba and Sr, is expected to be very resistant against crystallization (Kosmal et al. 2017). Of particular interest is however the white dotted pattern that was observed at the sample's top surface. The white substance – linked to surface crystallization was easily removed by submerging the sample into water.

A DSC analysis was conducted employing a STA 449 F3 Jupiter® apparatus. The test showed a stable glass with a shallow crystallization peak at around 700°C. Its glass transition temperature was found at the region of 550°C - 580°C. The stability of the glass and its high visual resulting quality prove the potential of this glass for casting glass building components.

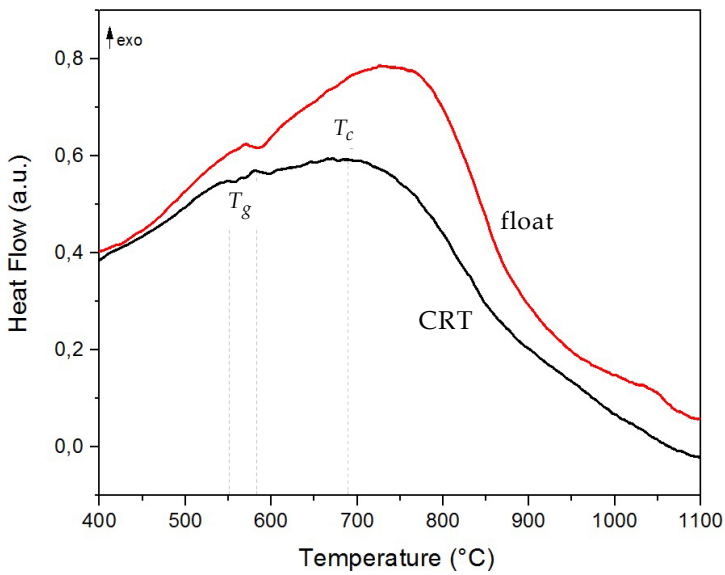

Figure 24. DSC analysis pointing out the glass transition temperature and crystallization peak temperature of the CRT sample. The temperature to heat flow curve of PPG Starphire float glass is included in the diagram as a point of reference.

The crystal traces on the top surface of the CRT sample kiln-cast at 970°C were isolated and XRF and XRD analyses were conducted. The XRF analysis showed a prevalence of sulfide, followed by alkali. The top surface crystallization can be therefore linked with the precipitation of these compounds during casting, in combination with the temperature occurring around the top surface. This crystallization is mainly considered as a flaw of the kiln-casting technique and is not expected in the melt-quenching casting process that takes place in atmospheric conditions. The XRD analysis showed four different crystalline phases, with Barium sulfate and the aphthitalite having the sharpest peaks. Aphthitalite, like other K-salts, is water soluble, explaining the easy removal of the crystallization skin from the sample, when immerged in water.

Table 2: XRF analysis of surface crystallization appearing on CRT panel glass sample kiln-cast at 970°C

Compound name	Content [wt%]
S	52.897
Na_2O	20.051
K_2O	17.43
BaO	4.832
SrO	4.162
SiO_2	0.177
Cl	0.146
CaO	0.110
MgO	0.067
Al_2O_3	0.052
Fe_2O_3	0.044
P_2O_5	0.032

Table 3: XRD analysis of surface crystallization appearing on CRT panel glass sample kiln-cast at 970°C

Crystalline phases	Compound
Barium sulphate (IV) sulphate (VI)	Ba(SO3)0.3(S04)0.7
Aphthitalite	KNa(SO4)
Disodium sulfate (VI)	Na2(SO4)
Kalistrontite	K2Sr(SO4)2

Firing set-up: Top temperature 970°C; Quench ramp 160°C/h

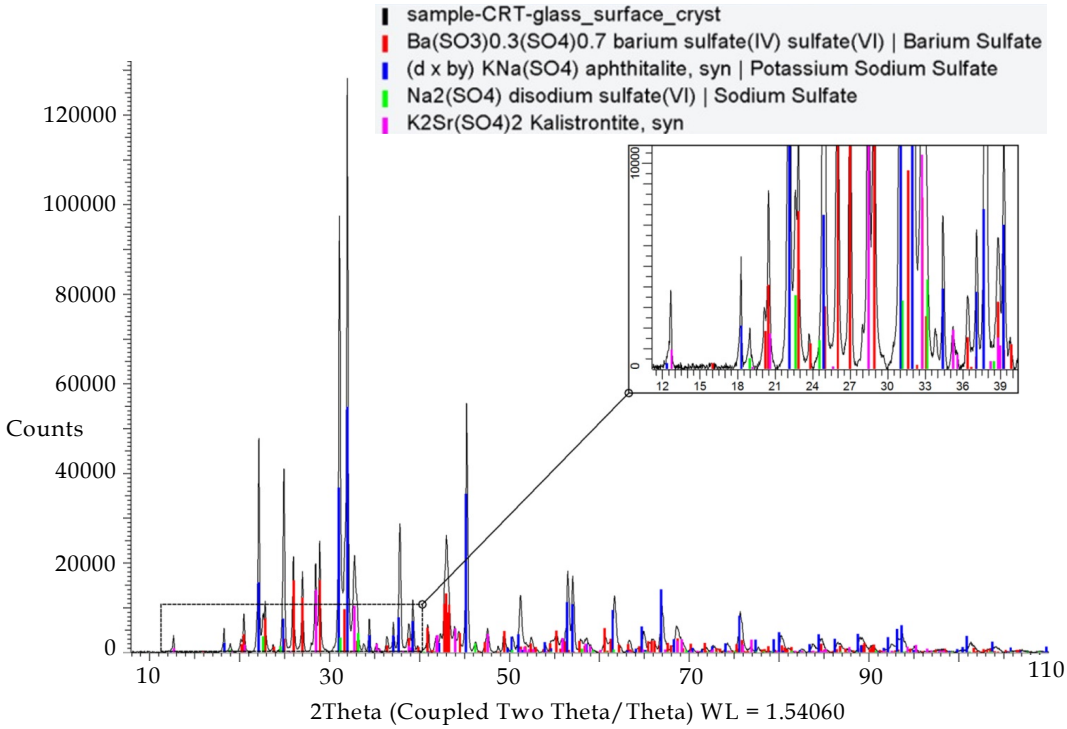

Figure 26: The XRD graph shows the measured patterns in black, after background subtraction. The coloured bars give the peak positions and intensities of the possibly present identified phases, using the ICDD pdf4 database

• *Borosilicate (laboratory tubes)*

Borosilicate glass can be attractive for structural applications at demanding environmental conditions, due to its good optical properties and its high thermal and chemical durability (Schott 2014b). It is commonly found in thermal shock resistant cookware and laboratory equipment. Its higher working temperature in comparison to that of soda-lime adds implications to its processing. Guidelines regarding recycling commonly advise not to discard borosilicate objects together with container glass. Unless chemically contaminated and thus hazardous, this good quality glass often ends up in landfills. Investigations for its downcycling into micro-filler for concrete (Korjakins et al. 2012), glass foams (Chinnam et al. 2014) and other ceramic material applications are currently conducted.

A piece of DURAN® laboratory glass produced by Schott was re-cast at 1200°C and resulted into a clear homogeneous glass after being abruptly cooled. The top surface was

Figure 27: Borosilicate labtube before and after casting at 1200°C

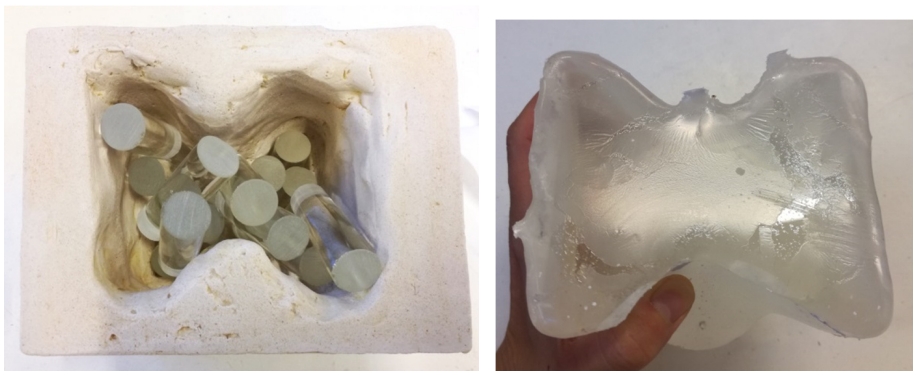

Figure 28: Borosilicate extruded rods successfully re-cast at 1120°C

completely flat and showed some local crystallization. DURAN® extruded solid rods by Schott were also successfully re-cast at 1120°C, using Crystalcast moulds within a heat-resistant concrete case. Despite the minimum surface crystallization appearing on this sample as well, the result was transparent and bubble free.

• *Alkali-aluminosilicate (mobile phone screen)*

Alkali-aluminosilicate glasses are characterized by high glass transition temperatures and excellent mechanical properties such as increased hardness, and scratch and sharp contact damage resistance (Corning 2017; Schott 2014b). Their high alkali content (>10%) enables the ion exchange with bigger alkali ions (ex. potassium bath) that results in a considerably improved surface compressive strength (Schott 2014b). This glass can be drawn via an automated process into very thin sheets of glass (0.4–2 mm) that find applications in the

screens of smartphones, laptops, tablets and other similar devices (Corning 2015). Due to its outstanding mechanical properties and the fact that touchscreens of that kind are an increasing upcoming source of glass waste, the recycling of alkali-aluminosilicate glass into building components becomes interesting. Yet, their extremely high working temperatures create challenges for hot-pouring and kiln-casting.

An initial test was conducted by melting a mobile phone screen glass in a high-alumina crucible. At 1500°C the sample still presented a very high viscosity, but some glass drops

a) Before firing

b) After firing at 1250°C

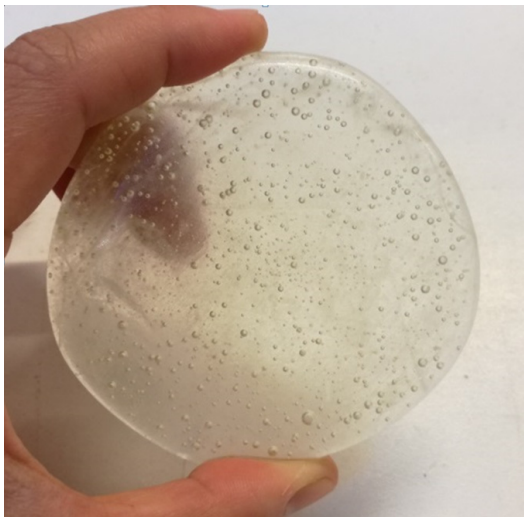

c) Kiln cast at 970°C

d) Melted at 1500°C in a high-alumina crucible and poured into a steel mould

Figure 29: Alkali-aluminosilicate glass retrieved from a mobile phone screen

managed to flow and resulted in a glass of high air-bubble content. The results of the kiln-casting test at 1250°C were quite unexpected as the glass partially corroded the silica-plaster mould and formed – probably as a reaction to the mould – a three-dimensional sponge structure of opaque white colour. Further testing is required to understand the reasons behind this foam formation. On the contrary, the sample kiln-cast at 970°C successfully formed a glass, although of high air-bubble content. Despite the air-bubbles, the formation of this glass at lower than 1000°C temperatures is very promising.

4 Conclusions and further research

The results of this research highlight the vast potential for recycling different types of discarded glass into cast glass building components. Products that are currently almost entirely excluded from the glass-to-glass recycling loop such as CRT panels or crystal tableware- both containing a considerable percentage of heavy metals- proved to be an excellent source of glass that can be kiln-cast at temperatures between 900°C - 1000°C. Soda-lime float, mouth-blown and container glasses, in comparison, needed higher

working temperatures (≈ 1200°C) and faster cooling rates to homogenize into transparent glass samples. Also, glasses from the same family and of similar colours are considered compatible for cast-recycling. The casting of glasses of the above family at temperatures below 1000°C combined with a slow cooling, showed an aesthetically and structurally interesting alternative route, that of glass ceramics. In this case, more investigation is required in order to control the desired percentage of crystalline phases within the material. The recycling of borosilicate laboratory glassware can result into very clear glass, and is worth considering despite of the higher than soda-lime required working temperatures. More investigation is required for the successful kiln-casting of Aluminosilicate glass. Initially, the difficulty to flow even at 1500°C renders this glass unsustainable for recycling through casting. Yet, the ability to form it at 970°C, even with a high content of gas-bubbles, seems promising and requires further testing.

The authors also suggest further research on the mixing of different glass recipes with the aim of simplifying the initial, meticulous stage of segregation of the cullet in fewer glass categories. Towards this step, a method should be developed for controlling the quality of the segregated cullet and thus the quality of the final product in terms of strength and aesthetic homogeneity. Future work will be conducted on the mechanical testing of the

Figure 30: The fundamental differences between various types of glass regarding viscosity, thermal expansion and susceptibility to crystallization, introduce challenges to their mixing. Further research should be conducted to overcome the posed obstacles.

resulting recycled glass components to define their strength and validate their suitability as building components. Research should also address the recycling of glass contaminated by coatings, laminates, and adhesives, which nowadays constitute a considerable amount of our glass waste. The above steps are necessary for diverting the path of waste glass from the landfills to safe and beautiful structures.

Figure 31: Successful casting of pieces of (from left to right) float glass, bottle, laboratory tube, computer screen panel, lens, and mouth blown glass, demonstrating the numerous possibilities that arise in creating unique building components

Acknowledgements

The authors would like to thank Prof. Jiyong Lee and Katherine Rutecki from the School of Art and Design at Southern Illinois University (SIU), and glass artist Joshua Hershman for their inspiring guidance and technical knowledge in kiln-casting. Ruud Hendrikx (3mE, TU Delft) was of significant help, providing with all the XRF and XRD analyses. We are also grateful to Lida Barou (CiTG, TU Delft), Mariska van der Velden (CiTG, TU Delft), Kees Baardolf (BK, TU Delft), Ron Penners (CiTG, TU Delft), and Tommaso Venturini (BK, TU Delft) for their valuable assistance in the TU Delft Glass Laboratory. Finally we would like to thank Annissa Flickinger Glenn Miner, Paul W. Bush, Patrick J. Kenny from Vitro Architectural Glass for providing us with glass samples and valuable input.

References

Abrisa Technologies: *Specialty Glass Materials Products & Specifications* (2014)

Bernando, E., Andreola, F., Barbieri, L. and Lancellotti, I.: Sintered Glass–Ceramics and Glass–Ceramic Matrix Composites from CRT Panel Glass. *Journal of the American Ceramic Society* 88 (7) (2005)

Bray, C.: *Dictionary of Glass: Materials and Techniques*, Second ed. A&C Black, London (2001)

Bristogianni, T., Oikonomopoulou, F., Veer, F.A., Snijder, A.H., and Nijsse, R.: Production and Testing of Kiln-cast Glass Components for an Interlocking, Dry-assembled Transparent Bridge. In: *Glass Performance Days*, Glaston Finland Oy, Tampere (2017)

Bristogianni, T., Oikonomopoulou, F., Justino de Lima, C., Veer, F.A. and Nijsse, R.: Cast Glass Components out of Recycled Glass: Potential and Limitations of Upgrading Waste to Load-bearing Structures. In: *Challenging Glass 6 Proceedings*, Delft (2018)

Brockway, M.C.: Fluid Bed Chemical Strengthening of Glass Objects. USA Patent 4290793 (1981)

Burch, O.G. and Badcock, C. L.: Effect of Glass Color on Setting Rates in Manufacture of Glass Bottles, *Journal of the American Ceramic Society* 21 (10) (1938)

Campbell, D.E. and Hagy, H.E.: Glass and Glass-Ceramics. In: Lynch, C.T. (ed.) CRC *Handbook of Materials Science*, Volume II: Metals, Composites and Refractory Materials. CRC Press, Florida (1990)

Chinnam, R.K., Molinaro, S., Bernardo, E. and Boccaccini, A.R.: Borosilicate Glass Foams from Glass Packaging Residues. In: Dogan, F., Tritt, T.M., Sekino, T., Katoh, Y., Pyzik, A.J., Belharouak, I., Boccaccini, A.R. and Marra, J. (ed.) *Ceramics for Environmental and Energy Applications* II. John Wiley & Sons, Inc., New Jersey (2014)

Clark-Monks, and Parker, J.M.: *Stones and Cord in Glass. Society of Glass Technology*, Sheffield (1980)

Compton, K.: *Image Performance in CRT Displays*. Spie Press Book (2003)

Cormier, L.: Chapter 1: The classical nucleation theory. In: Neuville, D.R., Cormier, L., Caurant, D., Montagne, L.: In: *Glass to Crystal: Nucleation, Growth and Phase Separation, from Research to Applications*. EDP Sciences, (2017)

Corning: Corning® Gorilla® Glass 3 (2015)

Corning: Corning® Gorilla® Glass 5 (2017)

Doremus, R.H.: *Glass Science*, 2nd ed. Wiley-Interscience (1994)

Dyer, T.D.: Chapter 14 - Glass Recycling. In: *Handbook of Recycling*. Elsevier, Boston (2014)

Edgar, R., Holcroft, C., Pudner, M. and Hardcastle, G.: UK Glass Manufacture. A Mass Balance Study. *CTS* (2008)

ELVIROS: Recycled Glass Market Study & Standards Review – 2004 Update (2004)

ESK: EKamold® Boron Nitride Sprays Release Agent and Protective Coating (2013)

Eurostat: Recycling rates for packaging waste (2016)

Gold Star: Gold Star Powders. www.siamcasting.com/download/SCP.pdf.

Heimerl, W.: Chemical Resistance and Corrosion, and Ion Release. In: Bach, H., and Krause, D. (ed.) *Analysis of the Composition and Structure of Glass and Glass Ceramics*. Springer-Verlag Berlin Heidelberg, New York (1999)

Holscher, H.H., Rough, R. R. and Plummer, J. H.: Experimental Studies of the Temperature Gradients in Glasses of Various Colors. *Journal of the American Ceramic Society* 26(12) (1943)

Hreglich, S., Falcone, R. and Vallotto, M.: The Recycling of End of Life Panel Glass from TV Sets in Glass Fibres and Ceramic Products. In: *Recycling and Reuse of Glass Cullet*. Thomas Telford Ltd., London (2001)

Karell, R., Kraxner, J., Chromèíková, M. and Liška, M.: *Properties of selected zirconia containing silicate glasses* II. Ceramics − Silikáty 51 (2007)

Kitaĭgorodskiĭ, I.I. and Solomin, N.W.: Rate of Setting of Glass During Working. Society of *Glass Technology Journal* 18, 323-335 (1934)

Knight optical: Technical / Sheet Glasses TSG-B270. http://www.knightoptical.com/technical-library/sheet-and-technical-glasses/.

Korjakins, A., Shakhmenko, G. and Bumanis, G.: Utilisation of Borosilicate Glass Waste as a Micro-Filler for Concrete. *Journal of Civil Engineering and Architecture* 6 (2012)

Kosmal, M., Reben, M., Pichniarczyk, P., Ziąbka, M. and Skrzypek, S.J.: Surface crystallization and phase evolution of $BaO–SrO–TiO_2–SiO_2–Al_2O_3$-based glass ceramics. *Journal of Thermal Analysis and Calorimetry* 130 (2017)

Martlew, D.: Viscosity of Molten Glasses. In: Pye, D., Joseph, I. and Montenero, A. (ed.) *Properties of Glass-Forming Melts*. CRC Press, Taylor & Francis Group, (2005)

Mear, F., Yot, P., Cambon, M. and Ribes, M.: The characterization of waste cathode-ray tube glass. *Waste Management* 26 (2006)

Müller, R., Zanotto, E.D. and Fokin, V.M.: Surface crystallization of silicate glasses: nucleation sites and kinetics. *Journal of Non-Crystalline Solids* 274, 208-231 (2000)

Nielsen, R.: Zirconium and Zirconium Compounds. In: *Ullmann's Encyclopedia of Industrial Chemistry*. Wiley-VCH Verlag GmbH & Co. KGaA, (2000)

Oikonomopoulou, F., Bristogianni, T., Veer, F., & Nijsse, R.: The construction of the Crystal Houses façade: challenges and innovations. *Glass Structures & Engineering*, 1-22 (2017)

Precision Glass and Optics: PPG-Starphire

Pye, L.D.: Glass-Forming Melts. In: Pye, D., Joseph, I. and Montenero, A. (ed.) *Properties of Glass-Forming Melts.* CRC Press, Taylor & Francis Group, (2005) Ransom & Randolph: R&R/Dentsply Form

Rosenhain, W.: *Glass Manufacture*. D. Van Nostrand Company, New York (1908)

Schott: Data Sheet LF5 (2014)

Schott: Technical Glasses, Physical and Technical Properties. Germany, (2014)

Schott: Duran Technical Data (2017)

Scoullos, M., Vonkeman, G.H., Thornton, I., and Makuch, Z.: Mercury – Cadmium - Lead *Handbook for Sustainable Heavy Metals Policy and Regulation*. Springer Science + Business Media, Dordrecht (2001)

Seward III, T.P. and Varshneya, A.K.: Inorganic Glasses: Commercial Glass Families, Applications, and Manufacturing Methods. In: Harper, C.A. (ed.) *Handbook of materials and product design*. McGraw-Hill, Inc., USA (2001)

Shelby, J.E.: *Introduction to Glass Science and Technology*. The Royal Society of Chemistry, Cambridge, UK (2005)

Silva, R.V., Brito, J., Lye, C., and Dhir, R.: The role of glass waste in the production of ceramic-based products and other applications: A review, vol. 167. (2017)

Singer, G.: Absorption of X-rays by Lead Glasses and Lead Barium Glasses. Research of the National Bureau of Standards 16 (1936)

Specialty Glass Products: PPG Starphire Soda Lime Glass. www.sgpinc.com.

Spruce Pine Batch: Cristalica

ZRCI: ZRCI SDS-0018 (2017)

Zschimmer, E.: *Chemical Technology of Glass*. Society of Glass Technology, Sheffield, UK (2013)

Appendix 1. Properties of various types of commercial glasses

Glass family	Lead crystal	Lead-free barium strontium		Soda-lime (mouth-blown)
Glass name	Scott LFS	CRT colour panel	Corning 9068 (Colour TV panel)	Cristalica, Spruce Pine
Young's modulus *E* in kN/mm^2	59			
Thermal expansion coefficient *a* (20°C; 300°C) in 10^{-6} K^{-1}	10,6	9,7-10,9	9,9	10
Density in g/cm^3	3,22	2,75-2,79	2,69	
Forming temperature (viscosity = log4 in dPas) in °C				995
Forming temperature (viscosity = log5 in dPas) in °C				879
Forming temperature (viscosity = log6 in dPas) in °C				792
Forming temperature (viscosity = log7,6 in dPas) in °C	585		688	692
Annealing point(viscosity = log13 in dPas) in °C	411	501	503	515
Strain point (viscosity = log14,5 in dPas) in °C			462	486
Sources	Schott 2014b	Mear et al. 2006 Shelby 2005	Campbell et al. 1990 Seward III et al. 2001	Spruce Pine Batch

Glass family	Soda lime (float)		Soda lime (glass bottles)	Soda-potash-lime
Glass name	PPG Starphire	Kimble R6	Common glass container	Scott B270
Young's modulus *E* in kN/mm^2	73.1		70-75	71.5
Thermal expansion coefficient *a* (20°C; 300°C) in 10^{-6} K^{-1}	9.03	9.3	9	9.4
Density in g/cm^3	2.5		2.52	2.55
Forming temperature (viscosity = log4 in dPas) in °C		984		1033
Forming temperature (viscosity = log5 in dPas) in °C		871		915
Forming temperature (viscosity = log6 in dPas) in °C		789		827
Forming temperature (viscosity = log7,6 in dPas) in °C	710	694		724
Annealing point(viscosity = log13 in dPas) in °C	547	527	548	541
Strain point (viscosity = log14,5 in dPas) in °C	513	486		511
Sources	Precision Glass and Optics Speciality Glass Products	Martiew 2005 Brockway 1981	Shelby 2005	Knight Optical

Glass family	Borosilicate		Alkali-Aluminosilicate	Alkaline Earth Aluminosilicate
Glass name	Schott Duran*	"Pyrex" KG-33	Corning Gorilla Glass 5	EZ-1
Young's modulus *E* in kN/mm^2	64		76.7	
Thermal expansion coefficient *a* (20°C; 300°C) in 10^{-6} K^{-1}	3.3	3.3	7.88	4.2
Density in g/cm^3	2.23	2.23	2.43	2.52
Forming temperature (viscosity = log4 in dPas) in °C	1260	1248		1204
Forming temperature (viscosity = log5 in dPas) in °C		1072		1094
Forming temperature (viscosity = log6 in dPas) in °C		946		1010
Forming temperature (viscosity = log7,6 in dPas) in °C	825	805	884	915
Annealing point(viscosity = log13 in dPas) in °C	560	565	623 (13.2 poises)	715
Strain point (viscosity = log14,5 in dPas) in °C	518	513	571 (14.7 poises)	670
Sources	Schott 2017 Abrisa Technologies 2014	Doremus 1994 Martlew 2005	Corning 2017	Doremus 1994 Martlew 2005

Appendix 2: Composition of selected waste glass by category (XRF analysis)

Blown, automated
Green beer bottle
(Stella)

Compound name	Content [wt%]
SiO_2	73.34
Na_2O	12.41
CaO	9.925
Al_2O_3	1.598
MgO	1.454
K_2O	0.517
Fe_2O_3	0.341
Cr_2O_3	0.175
BaO	0.055
TiO_2	0.051
S	0.029
MnO	0.026
PbO	0.018
SrO	0.016
P_2O_5	0.015
ZrO_2	0.014
ZnO	0.006
CuO	0.005
NiO	0.003
Rb_2O	0.002

Blown, automated
Green beer bottle
(Heineken)

Compound name	Content [wt%]
SiO_2	72.094
Na_2O	12.039
CaO	10.704
MgO	2.24
Al_2O_3	1.514
K_2O	0.419
Fe_2O_3	0.368
Cr_2O_3	0.208
MnO	0.169
S	0.056
TiO_2	0.047
Cl	0.039
BaO	0.029
SrO	0.019
ZrO_2	0.018
PbO	0.013
P_2O_5	0.011
ZnO	0.010
Rb_2O	0.002

Blown, automated
Light green wine bottle
(from USA)

Compound name	Content [wt%]
SiO_2	73.360
Na_2O	12.704
CaO	11.313
Al_2O_3	1.220
K_2O	0.455
MgO	0.382
Fe_2O_3	0.323
Cr_2O_3	0.051
TiO_2	0.047
S	0.043
BaO	0.021
Cl	0.017
ZrO_2	0.015
P_2O_5	0.015
MnO	0.012
SrO	0.011
PbO	0.005
ZnO	0.004
Rb_2O	0.001

Blown, automated *Clear wine bottle* *(Riesling)*	
Compound name	Content [wt%]
SiO_2	72.543
CaO	11.266
Na_2O	10.953
MgO	2.030
Al_2O_3	1.683
K_2O	0.689
P_2O_5	0.244
S	0.163
CeO_2	0.114
Fe_2O_3	0.071
TiO_2	0.065
BaO	0.048
MnO	0.034
Cl	0.030
SrO	0.021
ZrO_2	0.020
PbO	0.017
ZnO	0.012

Blown, automated *Clear* *(Coca cola)*	
Compound name	Content [wt%]
SiO_2	73.529
Na_2O	12.008
CaO	10.813
MgO	1.899
Al_2O_3	1.184
K_2O	0.211
S	0.168
Fe_2O_3	0.062
BaO	0.027
Cl	0.027
P_2O_5	0.021
PbO	0.020
SrO	0.013
ZrO_2	0.010
ZnO	0.008

Blown, automated *Clear* *(Spa)*	
Compound name	Content [wt%]
SiO_2	73.994
Na_2O	11.255
CaO	10.934
MgO	1.917
Al_2O_3	1.300
K_2O	0.225
S	0.121
Fe_2O_3	0.090
Cl	0.034
TiO_2	0.033
BaO	0.028
SrO	0.015
P_2O_5	0.015
ZrO_2	0.013
PbO	0.011
ZnO	0.006

Blown, automated
Wine bottle mix
Clear

Compound name	Content [wt%]
SiO_2	73.356
Na_2O	11.882
CaO	9.878
MgO	2.165
Al_2O_3	1.261
K_2O	0.639
SrO	0.203
BaO	0.184
S	0.143
ZrO_2	0.085
Fe_2O_3	0.069
TiO_2	0.045
Cl	0.031
ZnO	0.024
P_2O_5	0.021
PbO	0.013

Blown, automated
Wine bottle mix
Light blue

Compound name	Content [wt%]
SiO_2	72.628
Na_2O	11.761
CaO	9.746
MgO	3.129
Al_2O_3	1.603
K_2O	0.661
S	0.190
Fe_2O_3	0.144
TiO_2	0.049
Cl	0.026
P_2O_5	0.022
ZrO_2	0.017
ZnO	0.009
PbO	0.008
SrO	0.006

Blown, automated
Wine bottle mix
Light green

Compound name	Content [wt%]
SiO_2	73.358
CaO	11.888
Na_2O	11.477
Al_2O_3	1.305
MgO	1.013
K_2O	0.397
Fe_2O_3	0.257
TiO_2	0.073
Cr_2O_3	0.062
BaO	0.047
S	0.025
SrO	0.021
ZrO_2	0.020
Cl	0.018
PbO	0.016
ZnO	0.011
P_2O_5	0.010
Rb_2O	0.003

Blown, automated *Wine bottle mix* *Green*	
Compound name	Content [wt%]
SiO_2	71.124
Na_2O	12.903
CaO	11.072
Al_2O_3	2.875
K_2O	0.882
Fe_2O_3	0.446
MgO	0.239
Cr_2O_3	0.211
TiO_2	0.070
P_2O_5	0.045
Cl	0.044
S	0.038
BaO	0.025
SrO	0.017
ZrO_2	0.009

Blown, automated *Champagne glass*	
Compound name	Content [wt%]
SiO_2	73.241
Na_2O	12.862
CaO	10.883
Al_2O_3	1.621
MgO	1.277
S	0.149
TiO_2	0.052
Cl	0.027
K_2O	0.025
P_2O_5	0.022
ZrO_2	0.013
SrO	0.008

Mouth-blown *Spruce Pine* *Transparent blue*	
Compound name	Content [wt%]
SiO_2	71.768
Na_2O	14.288
CaO	6.834
Al_2O_3	2.306
CuO	2.038
Fe_2O_3	0.835
ZnO	0.759
K_2O	0.380
BaO	0.355
Sb_2O_3	0.161
MgO	0.133
ZrO_2	0.046
Co_3O_4	0.040
S	0.040
SrO	0.012
P_2O_5	0.005

Mouth-blown Spruce Pine Transparent orange	
Compound name	Content [wt%]
SiO_2	73.144
Na_2O	15.393
CaO	7.093
Al_2O_3	2.058
ZnO	0.886
BaO	0.411
K_2O	0.411
MgO	0.258
Sb_2O_3	0.223
Fe_2O_3	0.027
ZrO_2	0.024
S	0.023
PbO	0.021
SrO	0.012
Cl	0.010
P_2O_5	0.005

Mouth-blown Spruce Pine Transparent clear	
Compound name	Content [wt%]
SiO_2	74.610
Na_2O	13.595
CaO	7.356
Al_2O_3	2.037
ZnO	0.908
BaO	0.450
K_2O	0.388
Sb_2O_3	0.218
MgO	0.157
Er_2O_3	0.123
S	0.062
Fe_2O_3	0.054
Cl	0.016
SrO	0.013
P_2O_5	0.007
Ag_2O	0.005

Float glass PPG Starphire (extra clear)	
Compound name	Content [wt%]
SiO_2	74.563
Na_2O	13.323
CaO	8.905
MgO	3.006
S	0.105
Al_2O_3	0.035
Fe_2O_3	0.015
Cl	0.014
K_2O	0.012
P_2O_5	0.010
ZrO_2	0.007
SrO	0.005

Float glass
PPG clear

Compound name	Content [wt%]
SiO_2	74.214
Na_2O	12.438
CaO	10.029
MgO	2.859
Al_2O_3	0.142
Fe_2O_3	0.124
S	0.084
K_2O	0.043
P_2O_5	0.038
Cl	0.024
SrO	0.005

Float glass
PPG furnace waste
Aquamarine

Compound name	Content [wt%]
SiO_2	73.108
Na_2O	14.346
CaO	7.888
MgO	3.947
Al_2O_3	0.311
S	0.159
Fe_2O_3	0.087
K_2O	0.078
TiO_2	0.035
ZrO_2	0.014
Cl	0.013
P_2O_5	0.009
SrO	0.005

Float glass
PPG furnace waste
Light green

Compound name	Content [wt%]
SiO_2	67.410
Na_2O	13.676
Al_2O_3	8.828
CaO	5.943
ZrO_2	2.975
MgO	0.431
TiO_2	0.213
Fe_2O_3	0.171
S	0.101
SrO	0.089
K_2O	0.073
HfO_2	0.055
P_2O_5	0.020
Cl	0.015

Potash-soda-lime Optical Schott B270 lenses	
Compound name	Content [wt%]
SiO_2	71.802
Na_2O	10.138
K_2O	6.275
CaO	5.168
ZnO	2.198
Al_2O_3	2.083
TiO_2	1.765
Sb_2O_3	0.403
MgO	0.041
BaO	0.030
Cl	0.022
S	0.018
P_2O_5	0.017
Fe_2O_3	0.016
ZrO_2	0.008
SrO	0.006
Rb_2O	0.005
PbO	0.005

Potash-soda-lime Optical Czechoslovakian bowl	
Compound name	Content [wt%]
SiO_2	82.632
Na_2O	6.488
CaO	4.146
K_2O	3.200
MgO	2.755
SO_3	0.281
Al_2O_3	0.219
Cl	0.100
TiO_2	0.060
Fe_2O_3	0.045
PbO	0.028
P_2O_5	0.023
ZnO	0.010
ZrO_2	0.009
Rb_2O	0.004
Br	0.002

Lead Crystal Schott LF5	
Compound name	Content [wt%]
SiO_2	53.731
PbO	36.643
K_2O	5.387
Na_2O	3.771
Al_2O_3	0.198
SO_3	0.134
CaO	0.114
NiO	0.018
P_2O_5	0.005

Lead Crystal G210	
Compound name	Content [wt%]
PbO	47.002
SiO_2	44.714
K_2O	3.936
Na_2O	3.296
S	0.231
Pb_2O_3	0.215
CaO	0.212
Al_2O_3	0.203
Cl	0.086
MgO	0.060
Fe_2O_3	0.046

Lead Crystal D'Arques 24% Lead Bowl	
Compound name	Content [wt%]
SiO_2	63.229
PbO	24.799
K_2O	7.753
Na_2O	2.842
CaO	1.200
S	0.075
Al_2O_3	0.051
ZrO_2	0.026
Fe_2O_3	0.024

Alkali-barium silicate CRT computer screen (panel)	
Compound name	Content [wt%]
SiO_2	61.505
SrO	8.056
BaO	8.039
Na_2O	7.210
K_2O	6.776
ZrO_2	3.587
Al_2O_3	2.304
CaO	1.109
TiO_2	0.378
Sb_2O_3	0.343
MgO	0.296
SO_3	0.153
Fe_2O_3	0.095
CuO	0.055
Cl	0.028
ZnO	0.027
P_2O_5	0.023
NiO	0.018

Borosilicate *Schott lab glassware*		*Alkali-aluminosilicate* *Mobile phone screen* *thin glass*	
Compound name	Content [wt%]	Compound name	Content [wt%]
SiO_2	93.024 *	SiO_2	63.062
Na_2O	3.548	Al_2O_3	12.958
Al_2O_3	2.725	K_2O	11.120
K_2O	0.513	MgO	6.235
Cl	0.051	Na_2O	5.603
ZrO_2	0.049	ZrO_2	0.843
Fe_2O_3	0.036	CaO	0.062
TiO_2	0.033	S	0.039
P_2O_5	0.012	Fe_2O_3	0.027
ZnO	0.005	Cl	0.017
SrO	0.002	TiO_2	0.014
Rb_2O	0.002	HfO_2	0.013
		P_2O_5	0.006
		SrO	0.002

* Boron not traced, therefore, the Si content appears high.

Duran composition according to (Heimerl 1999) SiO_2 80, B_2O_3 13.